Proceedings of the 21st ICSMGE, Vienna, Austria, 14 – 19 June 2026. Pistrol, Adam & Schweiger (eds.)
Published by: ÖGG, Austrian Society for Geomechanics, Salzburg, Austria, ISBN 978-3-9503898-4-5
https://doi.org/10.53243/ICSMGE2026-182

A new non-equilibrium approach to soil freezing

Chenjie Ruan, Wojciech Solowski
Department of Civil Engineering, Aalto University, Finland, chenjie.ruan@aalto.fi, wojciech.solowski@aalto.fi

ABSTRACT: Numerical simulations of saturated soils typically assume local isothermal conditions, ignoring the temperature difference between water and soil particles. However, as the thermal conductivity and heat capacity of soil particles are very different compared to water, the temperature of soil particles may change faster than that of water. The presented study shows the effect of non-local isothermal conditions between water and soil particles on soil freezing. The analysis employs two-system heat transfer equations that incorporate temperature differences between the soil particles and water.

KEYWORDS: Ground freezing, local thermal nonequilibrium, saturated soil, frozen fringe, numerical modelling.

1 INTRODUCTION

Frost heave poses a significant challenge to infrastructure in cold regions, particularly to roads and railways. This phenomenon is driven primarily by moisture migration. It influences the service life and structural integrity. Frost heave has been extensively studied, including theoretical and numerical models by Miller (1972), Konrad & Morgenstern (1980), Rempel et al. (2004), and Nishimura et al. (2009). These commonly followed models adopt the local thermal equilibrium assumption, neglecting the temperature difference between water and soil particles. Then the heat transfer is described by a unified temperature field, which effectively reduces the computational complexity of phase transitions. However, Roshan et al. (2014) state that this assumption may not be applicable to fine-grained soil materials with low fluid velocities, as neglecting local thermal nonequilibrium may affect the correct estimation of pore water velocity and heat flux.

The experiments by Jia et al. (2019) demonstrate that during the freezing of sand, ice formation initiates on the surface of the soil particles. This is attributed to the higher thermal conductivity of the soil skeleton compared to water, which results in the particles maintaining a locally lower temperature than the surrounding pore water. Therefore, the water adjacent to the particles experiences local thermal non-equilibrium, cooling faster and forming an ice coating on the particle surfaces.

Considering the effect of local thermal nonequilibrium, Ruan et al. (2025) proposed a simple thermal-hydraulic soil freezing framework employing a two-system heat transfer approach. To describe the soil pore structures, they used the capillary bundle model, dividing the soil into five intervals with equivalent volume to track the change of soil properties relative to the change of soil pore structures during soil freezing. In this paper, we first validate the capability and applicability of this framework by replicating a one-dimensional soil freezing test. Additionally, a sensitivity analysis was carried out by setting the soil particle thermal conductivity to three discrete values to investigate the effect of soil thermal properties on freezing. Moreover, we applied different interval numbers in the capillary bundle model to assess their influence on the simulations.

2 THERMAL AND WATER TRANSFER

The soil freezing framework assumes a two-component representation of the material: a) water in two phases (liquid and solid), and b) soil in the solid phase. To perform thermal-hydraulic analysis, the framework adopts a two-system heat transfer method (Quintard & Whitaker, 1995; Roshan et al., 2014; Gossler et al., 2020) and Darcy's law. The framework relies on the links between grain size distribution, pore size distribution and pore space size changes during freezing for the estimation of hydraulic conductivity. The capillary bundle model (Watanabe & Flury, 2008; Heinze, 2021) is applied to capture the pore space changes during freezing.

2.1 *Capillary bundle model*

The capillary bundle model is a simplification of the soil matrix, usually used to estimate the pore size distribution of the soil (Watanabe & Flury, 2008). This method approximates the pore structure as a collection of parallel, cylindrical capillary tubes of different diameters, which is illustrated in Figure 1.

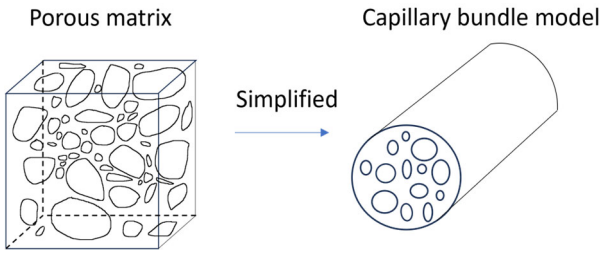

Figure 1. Illustration of the capillary bundle model

The total volume and surface area of pore space can be expressed as (Ruan et al., 2025):

$$V_{tube} = V_p = n\left(V_p + V_s\right) = \sum_{j=0}^{M} \pi R_j^2 N_j L\tau \qquad (1)$$

$$S_{tube} = \sum_{j=0}^{M} 2\pi R_j N_j L\tau \qquad (2)$$

Here, S_{tube} is the surface area of capillary tubes, V_{tube} is the total volume of capillary tubes, which is equal to the total volume of pore space V_p, V_s is the volume of soil particles, n is the porosity. L is the height of the tube, τ is the tortuosity of the tube. While $L\tau$ affect the number of capillaries per bundle, it has no impact on the specific surface area required for local heat transfer (see Section 2.2), which is defined as $\frac{S_{tube}}{V_{tube}}$. N is the number of capillaries of radius R in the bundle j, and M is the number of bundles used. Equations (1) and (2) allow us to calculate the surface area and volume of all tubes, meaning we can estimate the specific surface area of soil particles and the pore size distribution. More details can be found in Watanabe & Flury (2008).

2.1.1 *Influence of soil freezing on pore size distribution*

During freezing, liquid water on the surface of soil particles turns into ice, forming an ice coating around the soil particles. Thus, the effective pore radius of capillary tubes becomes smaller, reducing the contact area between unfrozen water and the solid phase, as shown in Figure 2.

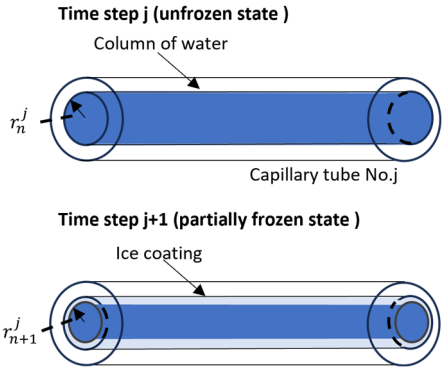

Figure 2. Illustration of the capillary tube (Ruan et al.,2025)

Equation (3) (Ruan et al., 2025) shows how the volume of unfrozen water changes with the degree of ice saturation S^i. Further, Equation (4) (Ruan et al., 2025) is applied to estimate the change of effective pore radius during freezing.

$$\frac{V_{unfrozen\ water}}{V_{single\ tube}} = \frac{\pi(R_j^{eff})^2 L\tau}{\pi(R_j)^2 L\tau} = S_j^l \tag{3}$$

$$R_j^{eff} = \sqrt{S_j^l} R_j \tag{4}$$

Here, the R_j^{eff} is the effective pore radius of the j-th capillary tube.

2.2 *Heat transfer equations*

Equation (5) and (6) shows the heat balance equations for soil and water separately (Ruan et al., 2025).

$$\rho_s c_s \frac{\partial \mathrm{T}_s}{\partial t} = \lambda_s \nabla \cdot \nabla T_s + \frac{a_{fs} h_{ht} (\mathrm{T}_w - \mathrm{T}_s)}{1-n} \tag{5}$$

$$n\frac{\partial H_w}{\partial t} = n\lambda_w \nabla \cdot \nabla T_w + a_{fs} h_{ht} (\mathrm{T}_s - \mathrm{T}_w) - \rho_w^l c_w^l \boldsymbol{q^l} \cdot \nabla T_w \tag{6}$$

Here, H_w is the enthalpy of the water. ρ_w^l is the liquid water density and ρ_s is soil density. c_w^l is the liquid water specific heat capacity and c_s is the soil specific heat capacity. T_s, T_w are the temperatures of soil (s) and water (w). λ_s, λ_w are the thermal conductivities of soil and water. a_{fs} is the specific surface area of the soil, h_{ht} is the heat transfer coefficient between liquid and solid material, and can be estimated based on the suggestions from Roshan et al. (2014). $\boldsymbol{q^l}$ is the liquid water velocity. For simplicity, we neglect the freezing point depression and assume all water will freeze at the same temperature 273.16K. To model the water-ice phase transition, we implement the enthalpy method that incorporates the latent heat into the total energy equation (Voller, 1997). When a phase transition occurs, the thermal conductivity of the water is:

$$\lambda_w = {\lambda_w^l}^{S^l} \cdot {\lambda_w^i}^{S^i} \tag{7}$$

Where $\lambda_w^{l,i}$ is the thermal conductivity of liquid water (l) and ice (i). $S^{l,i}$ is the degree of saturation of water (l) and ice (i).

2.3 *Water transfer equation*

The water transfer in the framework follows Darcy's law:

$$\frac{\partial \phi^w}{\partial t} + \nabla \cdot \boldsymbol{q^l} = 0 \tag{8}$$

Here, ϕ^w is the volume friction of the water, water flux $\boldsymbol{q^l}$ is proportional to the total hydraulic potential gradient:

$$\boldsymbol{q^l} = -k(\nabla h + 1) \tag{9}$$

Here h is the capillary suction, k is the hydraulic conductivity.

2.3.1 *Hydraulic conductivity*

The framework accounts for the thermal property difference between soil particles and water. It is designed for soils that are highly frost-susceptible and contain small amounts of fine particles. The framework assumes that the freezing process begins with the water on the surface of the soil particles. During freezing, an ice layer forms on the surface of the soil particles. Over time, this ice layer becomes thicker. The freezing process reduces the effective porosity, thereby reducing the hydraulic conductivity. The Carmen-Kozeny relation, combined with the capillary bundle model, is used to describe the changes in hydraulic conductivity (Ruan et al., 2025):

$$k = k_0 \sum_{j=0}^{M} w_j \frac{n_j^3}{(1-n_j)^2} \frac{(1-n_{ref})^2}{n_{ref}^3} \tag{10}$$

Here, k_0 is the hydraulic conductivity of saturated soil, n_{ref} is the referenced porosity of the soil, w_j represents the fractional contribution of bundle j to the total volumetric water flow rate, defined as the ratio of the water flow rate of each capillary bundle Q_j to the total water flow rate Q, and can be estimated based on the modified Hagen-Poiseuille equation derived by Watanabe & Flury (2008).

$$w_j = \frac{Q_j}{Q} = \frac{\frac{\pi \rho_w^l g}{8\mu}\frac{\Delta h}{L} N_j R_j^4}{\frac{\pi \rho_w^l g}{8\mu}\frac{\Delta h}{L} \sum_{j=1}^{M} N_j R_j^4} \tag{11}$$

where g denotes the gravity accelerations and μ stands for the water viscosity.

2.3.2 *Capillary rise*

The water migration driving force from unfrozen to freezing zones is assumed to be governed by the capillary rise. The air entry value is selected as the capillary rise value that acts at the frozen front.

3 VALIDATION AND NUMERICAL STUDIES

This paper replicates a one-dimensional soil freezing experiment on Devon silt from Konrad & Morgenstern (1981). The test uses a soil sample of 7.8cm in height. Before the test, they cooled the room and the soil sample temperature to 0.4°C. Further, it employs a constant low temperature at top and an above-zero temperature at the bottom of the samples with no externally applied load during the test. The details of the test conditions are shown in the Table 1. The experiment simulation uses the finite difference method to discrete the space and time. Spatial derivatives are approximated with a first-order forward difference scheme. By using the water retention curve of the Devon silt, as shown in Figure 3, based on Jurin's law, we convert Figure 3 into pore structure distributions and discretised it into several intervals (this paper used M=5 and 10) with an equivalent degree of saturation, and applied the capillary bundle model to consider the influence of the pore structure change during freezing. The curve shown in Figure 3 was estimated by the pedotransfer function (Scheinost et al., 1997) based on the soil particle grading curve provided by Xia et al. (2005). The soil parameters used are listed in Table 2.

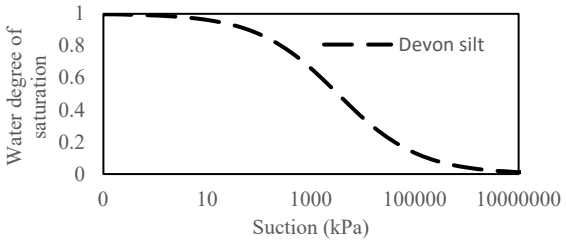

Figure 3. Water retention curve

Table 1. E4 Test conditions.

Parameter	Symbol	Value	Unit
Top temperature	T_{warm}	-5.5	°C
Bottom temperature	T_{body}	3	°C
Body temperature	T_{cold}	3	°C
Sample length	L	78	mm

Table 2. Parameters for Devon silt E4 test.

Parameter	Symbol	Value	Unit
Heat capacity of soil grains	c_s	900	J/kg/K
Heat capacity of water	c_w^l	2108	J/kg/K
Thermal conductivity of soil grains	λ_s	1.6	W/m/K
Thermal conductivity of ice	λ_w^i	2.18	W/m/K
Thermal conductivity of water	λ_w^l	0.56	W/m/K
Density of soil grains	ρ_s	1700	kg/m^3
Density of water	ρ_w^l	1000	kg/m^3
Porosity	n_{ref}	0.38	-
Saturated hydraulic conductivity	k_0	2.4E-7	cm/s
Air entry value	h	4.5	m

3.1 *Convergence study*

The mesh sensitivity analysis is shown in Figure 4. The calculations used the element lengths of 0.5mm, 0.25mm, 0.125mm and 0.0625mm for the one-dimensional soil freezing test. This study indicated that the element length of 0.125mm gives solutions that are accurate enough for this case. Therefore, all results shown in Section 3.2 are simulated with this size.

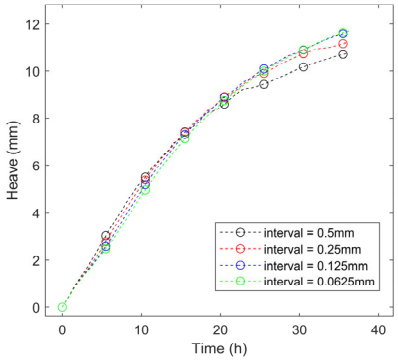

Figure 4. Heave amount simulated with different element lengths

3.2 *Results*

3.2.1 *Frost heave*

The results of frost heave variation during freezing are shown in Figure 5. It indicates that all the simulations replicate the measured frost heave qualitatively well. Comparing the frost heave of different bundle numbers at 35 hours, the results show that the differences are minor (see Table 3). The capillary bundle model simplifies the description of soil pore structures. The number of bundles influences the model's estimation of soil pore volume; more bundles can more accurately describe the soil pore structures, enabling more precise estimation of related parameters (e.g., hydraulic conductivity). However, the deviation shown in Table 3 indicates that while increasing the number of bundles can further improve simulation accuracy, the results at M =5 are already sufficiently accurate. Considering that the computational costs for M =10 are 3–4 times those for M =5, we believe that using M =5 for simulation calculations is an appropriate choice.

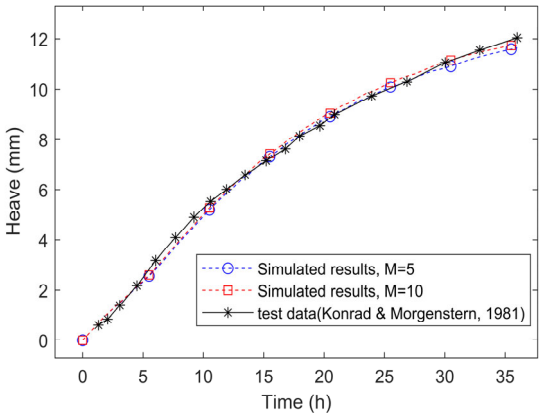

Figure 5. The frost heave variation during freezing

Table 3. Deviation caused by different bundle numbers.

Bundle numbers	Frost heave(mm)	Deviation compared to the test data
M =5	11.65	3.3%
M =10	11.77	2.3%

3.2.2 *Frozen front*

Figure 6 shows the change of the Frozen front position during soil freezing. The simulation results are in good agreement with the measured data, though a slight deviation in the predicted frozen front position is evident. This deviation is due to the assumption that all pore water freezes at the same temperature. Actual soil freezing involves freezing point depression caused by many factors, such as salinity, pressure, and chemical reactions between soil particles and water. Therefore, some unfrozen water may still exist in the soil, and our model, which assumes that unfrozen water does not exist, consumes additional energy in the simulation for the phase change of the water. As a result, there is a slight deviation between the measured and simulated frozen front position. Further increasing the bundle numbers does not affect the position of the frozen front.

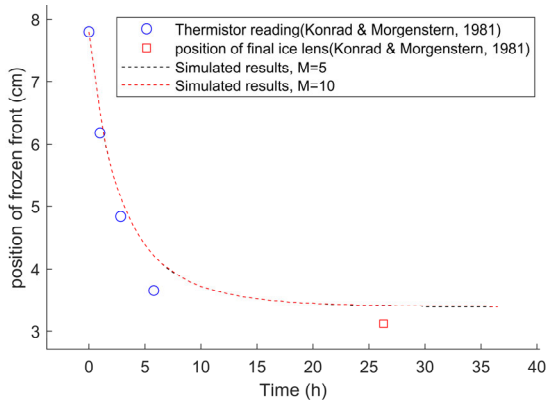

Figure 6. Frozen front variation during freezing

3.2.3 *Frozen fringe thickness*

The frozen fringe thickness due to the temperature difference between the soil particles and water is simulated and shown in Figure 7. Here, we investigated how the different thermal conductivities of soil particles affect the thickness of the frozen fringe. At the start of freezing, the initial freezing fringe is thicker due to the larger temperature difference between the solid particles and the water at the frozen front, and the higher thermal conductivity of soil particles a thicker frozen fringe. As freezing continues, the temperature gradient at the freezing front decreases, which also means that the temperature difference between the soil particles and the water becomes smaller, leading to a decrease in the thickness of the frozen fringe. When the temperature gradient is close to the quasi-steady state, the temperature difference between the soil particles and the water is negligible, and the frozen fringe due to local thermal non-equilibrium becomes minimal.

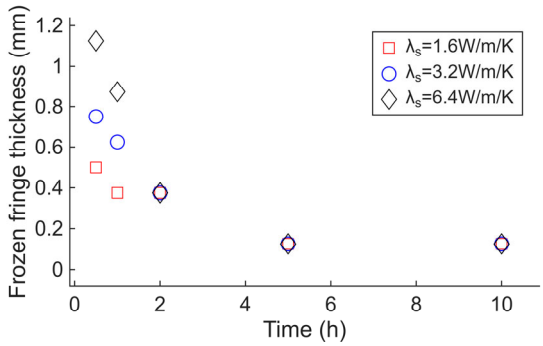

Figure 7. Frozen fringe thickness

4 CONCLUSION

The paper investigates the effect of local thermal non-equilibrium in soil freezing by using a two-system heat approach. The capillary bundle model has been applied to illustrate the soil pore structures and track the change of soil properties due to pore structure variation. The successful replication of the one-dimensional soil freezing test validates the new approach. The result suggests that the local thermal non-equilibrium affects the frozen fringe thickness, especially at the beginning of the experiments, before reaching steady state. The thermal properties difference between soil particles and water creates an area where the water temperature is higher than the freezing point, while the soil particle temperature is below the freezing point. In this area, phase transition appears due to local thermal non-equilibrium, creating a frozen fringe, which is strongly affected by the thermal properties of soil particles. Therefore, neglecting local thermal non-equilibrium during the initial freezing stage leads to significant uncertainty in predicting heat transfer within the soil.

Moreover, the paper studies the influence of the bundle numbers in the capillary bundle model. The results indicate that increasing the number of bundles does not significantly improve the accuracy. Therefore, M =5 is an appropriate option when applying the capillary bundle model during soil freezing simulations.

5 ACKNOWLEDGEMENTS

The authors would like to sincerely acknowledge the funding of this study by the Project DeMiCo, supported by Decarbonized Cities Business Finland financing, and the Aalto University School of Engineering Dean's scholarship.

6 REFERENCES

Gossler, M. A., Bayer, P., Rau, G. C., Einsiedl, F., & Zosseder, K. (2020). On the limitations and implications of modeling heat transport in porous aquifers by assuming local thermal equilibrium. Water Resources Research, 56(10), e2020WR027772.

Heinze, T. (2021). A multi-phase heat transfer model for water infiltration into frozen soil. Water Resources Research, 57(10), e2021WR030067.

Jia, H., Ding, S., Wang, Y., Zi, F., Sun, Q., & Yang, G. (2019). An NMR-based investigation of pore water freezing process in sandstone. Cold Regions Science and Technology, 168, 102893.

Konrad, J.-M., & Morgenstern, N. R. (1980). A mechanistic theory of ice lens formation in fine-grained soils. Canadian Geotechnical Journal, 17(4), 473–486.

Konrad, J.-M., & Morgenstern, N. R. (1981). The segregation potential of a freezing soil. Canadian Geotechnical Journal, 18(4), 482–491. https://doi.org/10.1139/t81-059

Miller, R. D. (1972). Freezing and heaving of saturated and unsaturated soils. Highway Research Record, 393(1), 1–11.

Nishimura, S., Gens, A., Olivella, S., & Jardine, R. J. (2009). THM-coupled finite element analysis of frozen soil: formulation and application. Géotechnique, 59(3), 159–171.

Quintard, M., & Whitaker, S. (1995). Local thermal equilibrium for transient heat conduction: theory and comparison with numerical experiments. International Journal of Heat and Mass Transfer, 38(15), 2779–2796.

Rempel, A. W., Wettlaufer. S. J, & WORSTER, M. G. (2004). Premelting dynamics in a continuum model of frost heave. Journal of Fluid Mechanics, 498, 227–244. https://doi.org/DOI: 10.1017/S0022112003006761

Roshan, H., Cuthbert, M. O., Andersen, M. S., & Acworth, R. I. (2014). Local thermal non-equilibrium in sediments: Implications for temperature dynamics and the use of heat as a tracer. Advances in Water Resources, 73, 176–184. https://doi.org/https://doi.org/10.1016/j.advwatres.2014.08.002

Ruan, C., A. Gupta, & Sołowski, W. T. (2025). A Two-System Heat Transfer Approach to Soil Freezing: Numerical simulation of frost heave considering local thermal non-equilibrium effects [Manuscript submitted for publication]. Department of civil engineering, Aalto univeristy.

Scheinost, A. C., Sinowski, W., & Auerswald, K. (1997). Regionalization of soil water retention curves in a highly variable soilscape, I. Developing a new pedotransfer function. Geoderma, 78(3–4), 129–143.

Voller, V. R. (1997). An overview of numerical methods for solving phase change problems. Advances in Numerical Heat Transfer, 1(9), 341–380.

Watanabe, K., & Flury, M. (2008). Capillary bundle model of hydraulic conductivity for frozen soil. Water Resources Research, 44(12).

Xia, D., Arenson, L. U., Biggar, K. W., & Sego, D. C. (2005). Freezing process in Devon silt-using time-lapse photography. In 58th Canadian geotechnical conference, saskatoon, saskatchewan.